Optimizing the excitation of surface plasmon polaritons by difference-frequency generation on a gold surface

A. T. Georges* and N. E. Karatzas
Department of Physics, University of Patras, Patras 26500, Greece
(Received 16 January 2012; published 23 April 2012)

We investigate theoretically the excitation of surface plasmon polaritons (SPPs) by difference-frequency generation on a planar air-gold interface. Calculations are presented for three SPP wavelengths: 1.55 μm, 1.00 μm, and 750 nm (free-space values). The predicted conversion efficiency, optimized with respect to the angles of incidence of the two p-polarized laser pumps, increases by two orders of magnitude, from 3.5×10^{-8} at the telecom wavelength to 3.4×10^{-6} at 750 nm. The latter value is four orders of magnitude larger than the recently reported experimental value for SPP excitation at 633 nm by four-wave mixing. Higher conversion efficiency is expected at shorter SPP wavelengths before the efficiency will drop in the reflection edge of gold.

DOI: 10.1103/PhysRevB.85.155442 PACS number(s): 73.20.Mf, 78.68.+m, 42.65.Ky, 42.65.Tg

I. INTRODUCTION

The nonlinear optical excitation of monochromatic surface plasmon polaritons (SPPs), which was first proposed some 35 years ago,[1] has attracted renewed attention in recent years[2–5] due to potential applications in the fields of nanophotonics and ultrafast active plasmonics.[6–10] SPPs are transverse-magnetic-guided electromagnetic waves along a metal-dielectric interface, with transverse confinement on a nanometric scale and submillimeter absorption length at optical and near-infrared frequencies. The inherent coupling of these waves to conduction electrons in good free-electron metals, which support SPPs and give them these characteristics, offers a probe into the state of this extremely dissipative medium. Any change in the electronic polarization and, hence, the complex dielectric function of the metal will be reflected in the propagation characteristics of the SPPs. Therefore, the study of nonlinear optical excitation of SPPs is of interest not only for applications in the fields of active plasmonics and nanophotonics, but also for the basic physics of metal-surface nonlinear interaction with laser fields. Noncollinear laser beam mixing on a metal surface allows the launching of SPPs anywhere on a metal-air interface, without the need of coupling prisms or diffraction gratings for wave-vector matching. This is a useful tool for nonobstructive, *in situ* microscopy of metallic surfaces and nanostructures.[8,9] Two different techniques have been demonstrated in recent experiments on planar gold surfaces. The first one,[2] which employs four-wave mixing (FWM), has a reported intensity conversion efficiency of about 4×10^{-10} at laser pump intensities of about 20 GW/cm^2 for SPP generation at 633 nm with a response time of $\sim$7.9 fs.[5] The second one,[3] which employs laser-induced thermal gratings, has a much greater conversion efficiency of about 10^{-4} at similar laser intensities, but has picosecond medium-recovery (electron cooling) times. One way to increase the conversion efficiency, and still have a fast femtosecond response time, is to employ a second-order (three-wave mixing) coherent process, namely, difference-frequency generation (DFG). Note that wave-vector matching for SPP excitation is not feasible in the case of sum-frequency generation, which instead can be enhanced if one of the two summed waves is an SPP.[11] DFG is characterized by a $\chi^{(2)}$ nonlinear susceptibility,[12,13] and is more efficient than FWM at laser pump intensities below the damage threshold for a gold surface. In fact, DFG is the process considered in Ref. 1 for exciting surface phonon polaritons or exciton polaritons in materials with a $\chi^{(2)}$ of bulk origin. As is well known,[14] in the case of noble metals and for laser pump wavelengths greater than the value ($\lambda \geqslant 690$ nm for Au) below which strong one-photon absorption from the filled lower d band to the s conduction band starts to take place, the nonlinear susceptibilities are predominately of surface origin and the dominant second-order element is $\chi^{(2)}_{zzz}$, where z is the axis normal to the surface. This has been verified again in recent experiments on second-harmonic generation (SHG) in reflection from a gold surface using 810 and 1064 nm laser pumps.[15,16] In this paper, we investigate theoretically SPP excitation on a gold surface by DFG and present calculations for SPPs in the red and near-infrared region of the spectrum. The predicted conversion efficiency at the laser intensity mentioned above increases by two orders of magnitude, from 3.5×10^{-8} at the telecom wavelength of 1.55 μm to 3.4×10^{-6} at 750 nm.

II. THEORETICAL MODEL

Consider two p-polarized laser beams with frequencies ω_1 and ω_2 incident, as shown in Fig. 1, on a gold surface in the same plane of incidence. In practice, the two beams could be focused by cylindrical lenses, so as to have a millimeter-long interaction length on the metal surface.[17] The angles of incidence, θ_1 and θ_2, are adjusted so that the DFG process $\omega_3 = \omega_1 - \omega_2$ with wave vector $k_3 = k_1 \sin\theta_1 - k_2 \sin\theta_2$ is phase matched to the SPP on the air-gold interface. Since the thickness of the surface layer that is nonlinearly polarized by the laser beams is much smaller than the transverse localization width of the SPPs, the polarized layer can be treated as a sheet at $z = 0_-$, just inside the metal surface. In the plane-wave approximation, the nonlinear polarization at ω_3 is of the form

$$\mathbf{P}^{(2)}_3(x,z,t) = \mathcal{P}^{(2)}_{3z,s}\delta(z-0_-)e^{i(\omega_3 t - k_3 x)}\hat{z} + \text{c.c.}, \qquad (1)$$

where $\mathcal{P}^{(2)}_{3z,s} = \epsilon_0 \chi^{(2)}_s(\omega_3)\mathcal{E}_{1z}\mathcal{E}^*_{2z}$, with $\chi^{(2)}_s(\omega_3) = \int \chi^{(2)}_{zzz}(\omega_3)dz$ being the effective surface nonlinear susceptibility, while $\mathcal{E}_{1z} = (1+\varrho_1)\sin\theta_1\mathcal{E}_1$ and $\mathcal{E}_{2z} = (1+\varrho_2)\sin\theta_2\mathcal{E}_2$ are the complex amplitudes of the total z component of the two external electric fields at $z = 0_+$, and $\mathcal{E}_1, \mathcal{E}_2$ are the amplitudes of the incident fields. The Fresnel reflection coefficients are given by $\varrho_i = [n(\omega_i)\cos\vartheta_i - \cos\vartheta_t]/[n(\omega_i)\cos\vartheta_i + \cos\vartheta_t]$,

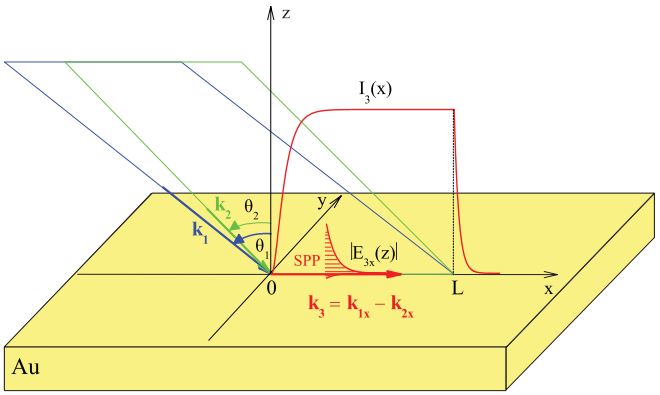

FIG. 1. (Color online) Schematic diagram for SPP excitation on a gold surface by difference-frequency generation. $\mathbf{k}_1$ and $\mathbf{k}_2$ are the wave vectors of the two incident laser beams, and $\mathbf{k}_3$ is that of the excited SPP. The curve labeled $I_3(x)$ shows the growth and decay of the plasmonic intensity with x, while $|E_{3x}(z)|$ displays the transverse localization of this surface-guided wave.

for $i = 1,2$, where $n(\omega)$ is the complex index of refraction of the metal and ϑ_t is the complex angle of refraction. The nonlinear polarization gives rise to an SPP of the form

$$\mathbf{E}_3(x,z,t) = \mathcal{A}_3(x)\boldsymbol{\mathcal{E}}_3(z)e^{i(\omega_3 t - k_{spp}x)} + \text{c.c.}, \tag{2}$$

where $\mathcal{A}_3(x)$ is a complex, slowly varying, dimensionless amplitude, and $\boldsymbol{\mathcal{E}}_3(z)e^{i(\omega_3 t - k_{spp}x)}$ is the solution of the homogeneous wave equation, with k_{spp} being the wave vector of the SPP. The vector amplitude $\boldsymbol{\mathcal{E}}_3(z)$ is given by[12]

$$\boldsymbol{\mathcal{E}}_3(z) = \begin{cases} [\mathcal{E}_{3x,d}\hat{x} + \mathcal{E}_{3z,d}\hat{z}]e^{-\alpha_d z}, & z > 0, \\ [\mathcal{E}_{3x,m}\hat{x} + \mathcal{E}_{3z,m}\hat{z}]e^{\alpha_m z}, & z < 0. \end{cases} \tag{3}$$

Substitution into the homogeneous wave equation gives the relations $k_{spp}^2 - \alpha_m^2 = (\omega_3/c)^2\epsilon_m$ and $k_{spp}^2 - \alpha_d^2 = (\omega_3/c)^2\epsilon_d$, where ϵ_m and ϵ_d are the relative permittivities of the metal and the dielectric, respectively, at ω_3. In order to satisfy Gauss's law, $\nabla\cdot[\boldsymbol{\mathcal{E}}_3(z)e^{i(\omega_3 t - k_{spp}x)}] = 0$, in each medium, the x and z components of the electric field must be related according to $\mathcal{E}_{3z,d} = -i(k_{spp}/\alpha_d)\mathcal{E}_{3x,d}$ and $\mathcal{E}_{3z,m} = i(k_{spp}/\alpha_m)\mathcal{E}_{3x,m}$. By applying boundary conditions on the x and z components of $\boldsymbol{\mathcal{E}}_3(z)$ at $z = 0$, one obtains the system of homogeneous equations

$$\mathcal{E}_{3x,d} - \mathcal{E}_{3x,m} = 0, \tag{4}$$

$$\epsilon_d\alpha_m\mathcal{E}_{3x,d} + \epsilon_m\alpha_d\mathcal{E}_{3x,m} = 0, \tag{5}$$

whose determinant is $D = \epsilon_m\alpha_d + \epsilon_d\alpha_m$. The root of D is the well-known dispersion relation for SPPs,

$$k_{spp} = k'_{spp} - ik''_{spp} = \frac{\omega_3}{c}\sqrt{\frac{\epsilon_d\epsilon_m}{\epsilon_d + \epsilon_m}}. \tag{6}$$

Substituting Eqs. (1) and (2) into the inhomogeneous wave equation,

$$\left[\nabla^2 - \frac{\epsilon_i}{c^2}\frac{\partial^2}{\partial t^2}\right]\mathbf{E}_3(x,z,t) = \mu_0\frac{\partial^2}{\partial t^2}\mathbf{P}_3^{(2)}(x,z,t), \tag{7}$$

where $\epsilon_i = \epsilon_d$ for $z > 0$ and $\epsilon_i = \epsilon_m$ for $z < 0$, we obtain in the slowly varying amplitude approximation the equation

$$i2k_{spp}\boldsymbol{\mathcal{E}}_3(z)\frac{d\mathcal{A}_3}{dx} = \mu_0\omega_3^2\mathcal{P}_{3z,s}^{(2)}\delta(z - 0_-)e^{i(k_{spp} - k_3)x}\hat{z}. \tag{8}$$

The nonlinear polarization couples to the z component of $\mathbf{E}_3$, and the product $\dot{\mathbf{P}}_3^{(2)}\cdot\mathbf{E}_3$ gives the power flow per unit volume from the former to the latter. Taking the scalar product of both sides of the equation above with $\boldsymbol{\mathcal{E}}_3^*(z)$, and then integrating over z, leads to

$$w|\mathcal{E}_{3z,d}|^2\frac{d\mathcal{A}_3}{dx} = -i\frac{\mu_0\omega_3^2}{2k_{spp}}\mathcal{P}_{3z,s}^{(2)}\mathcal{E}_{3z,m}^*e^{(i\Delta k + k''_{spp})x}, \tag{9}$$

where $\Delta k = k'_{spp} - k_3$ is the wave-vector mismatch of the DFG process, and

$$w = \left[2 - \frac{|\epsilon_d + \epsilon_m|}{|\epsilon_m|}\right]\frac{1}{\alpha_d + \alpha_d^*} + \left[2 - \frac{|\epsilon_d + \epsilon_m|}{|\epsilon_d|}\right] \times \frac{|\epsilon_d|^2/|\epsilon_m|^2}{\alpha_m + \alpha_m^*} \tag{10}$$

is the effective localization width of $|\boldsymbol{\mathcal{E}}_3(z)|^2$ at the dielectric-metal interface, which for $|\epsilon_m| \gg |\epsilon_d|$ reduces to $w \simeq 1/(\alpha_d + \alpha_d^*)$. Integrating Eq. (9) over x with the initial condition $\mathcal{A}_3(0) = 0$, we end up with

$$\mathcal{A}_3(x)\mathcal{E}_{3z,d} = -i\frac{\mu_0\omega_3^2}{2k_{spp}w}\frac{\epsilon_d^*}{\epsilon_m^*}\mathcal{P}_{3z,s}^{(2)}\frac{[e^{i\Delta kx}e^{k''_{spp}x} - 1]}{i\Delta k + k''_{spp}}. \tag{11}$$

The peak intensity of the excited SPP occurs on the dielectric side of the interface at $z = 0_+$, and is given by $I_3(x) = -2\text{Re}[E_{3z}H_{3y}^*]$, where $H_{3y} = (i/\mu_0\omega_3)[\partial E_{3x}/\partial z - \partial E_{3z}/\partial x]$ is the transverse-magnetic field. Carrying out the calculation, the peak intensity can be written in the form

$$I_3(x) = \epsilon_0\epsilon_d\omega_3 k'_{spp}\frac{|\epsilon_d + \epsilon_m|^2}{2|\epsilon_m|^4}\frac{\left|\mathcal{P}_{3z,s}^{(2)}/\epsilon_0\right|^2}{w^2[(\Delta k)^2 + (k''_{spp})^2]} \times |1 - e^{-i\Delta kx}e^{-k''_{spp}x}|^2, \tag{12}$$

where $0 \leqslant x \leqslant L$ lies in the illuminated area. Outside this area, for $x > L$, the intensity decays exponentially according to $I_3(x) = I_3(L)e^{-x/L_{spp}}$, where $L_{spp} = 1/(2k''_{spp})$ is the absorption length of the SPPs. As seen in Fig. 1, the plasmonic amplitude in the two areas rises and falls exponentially with the same characteristic length, $L_{spp}/2$ (much like the voltage vs time across a charging/discharging capacitor). The maximum value of $I_3(x)$ in the illuminated area for $x \gg L_{spp}$ turns out to be a few percent smaller than the value obtained when we apply the same theoretical treatment to the nonlinear polarization sheet, as in Ref. 5. The difference seems to be due to the averaging over z in obtaining Eq. (9) from Eq. (8) above. However, the present treatment has the advantage of giving the evolution of the peak SPP intensity with x, as well as its dependence on the various parameters explicitly, rather than in terms of the value of $|D|^2$ under phase-matching conditions. Note that for $\Delta k = 0$ and $x \gg L_{spp}$, Eq. (12) gives $I_3 \propto \omega_3 k'_{spp}|\chi_s^{(2)}(\omega_3)|^2 I_1 I_2 (L_{spp}/w)^2$, where $I_i = 2c\epsilon_0|\mathcal{E}_i|^2$ $[i = 1,2]$ are the intensities of the incident laser beams. The last factor in parentheses shows that the effect of the rapidly decreasing absorption length with increasing ω_3

is countered, though not completely, by the tighter transverse confinement (smaller w) of the SPPs. For example, in the case of gold for λ_3 in the range from 1550 to 750 nm, L_{spp}^2 decreases by a factor of 86, while the ratio $(L_{spp}/w)^2$ decreases only by a factor of 3.5. Nonetheless, because of the factor $\omega_3 k'_{spp}$ in front, the conversion efficiency is expected to be higher in the red than in the infrared region of the spectrum. Of course, the frequency dependence of $\epsilon_m(\omega_3)$, $\varrho_1(\omega_1)$, $\varrho_2(\omega_2)$, and $\chi_s^{(2)}(\omega_3;\omega_1,\omega_2)$ makes the overall frequency dependence of I_3 quite complicated, and numerical calculations are required in order to see the trends.

III. RESULTS AND DISCUSSION

Calculations have been carried out for the following three combinations of pump wavelengths: (i) $\lambda_1 = 800$ nm and $\lambda_2 = 1.653$ μm, generating the telecom wavelength $\lambda_3 = 1.55$ μm, (ii) $\lambda_1 = 700$ nm and $\lambda_2 = 2.3$ μm, generating $\lambda_3 = 1.00$ μm, and (iii) $\lambda_1 = 700$ nm and $\lambda_2 = 10.6$ μm, generating $\lambda_3 = 750$ nm. The three curves in Fig. 2 give the sets of angles (θ_1,θ_2) at which phase matching ($\Delta k = 0$) is achieved for SPP launching in the positive x direction. The values for the dielectric function of gold have been calculated from the tables for the complex index of refraction in Ref. 18. The points on the curves marked by open circles correspond to the optimum sets of angles, $(71.50^\circ, 62.70^\circ)$, $(72.75^\circ, 55.86^\circ)$, and $(63.10^\circ, -80.56^\circ)$, for maximum SPP peak intensity at $\lambda_3 = 1.55$ μm, 1.00 μm, and 750 nm, respectively.

Figure 3 shows the dependence of the peak SPP intensity I_3 for $x \gg L_{spp}$ on the angle θ_1, for the points on the phase-matching curve in Fig. 2 corresponding to $\lambda_3 = 1.55$ μm. In all calculations, the intensities of the pump

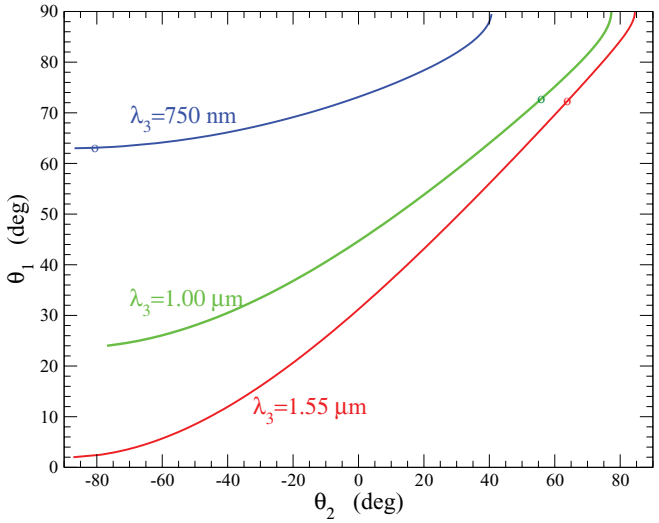

FIG. 2. (Color online) Plot of the sets of angles of incidence, (θ_1,θ_2), for which phase matching of SPP excitation by difference-frequency generation, $\omega_3 = \omega_1 - \omega_2$, is achieved. The three curves from the bottom up correspond to the cases (i) $\lambda_3 = 1.55$ μm, with $\lambda_1 = 800$ nm and $\lambda_2 = 1.653$ μm, (ii) $\lambda_3 = 1.00$ μm, with $\lambda_1 = 700$ nm and $\lambda_2 = 2.3$ μm, and (iii) $\lambda_3 = 750$ nm, with $\lambda_1 = 700$ nm and $\lambda_2 = 10.6$ μm. The open circles on the curves mark the optimum sets of angles for maximum conversion efficiency.

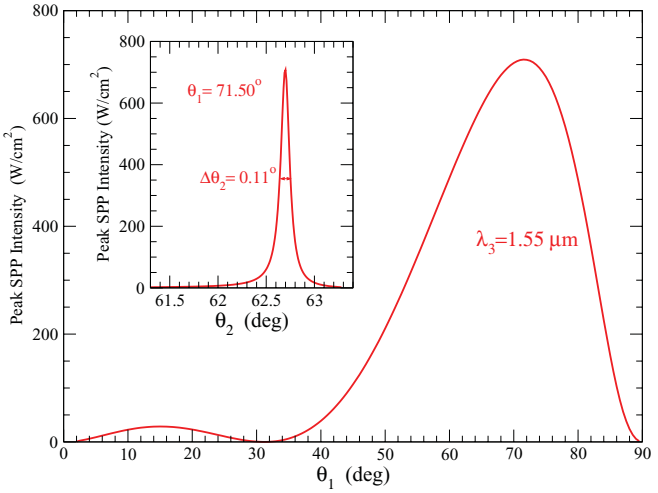

FIG. 3. (Color online) Plot of the peak SPP intensity vs the angle θ_1 along the corresponding phase-matching curve in Fig. 2 for $\lambda_3 = 1.55$ μm. The inset shows the peak SPP intensity vs the angle θ_2, with θ_1 fixed at the optimum value of 71.50 °.

laser beams are set both equal to 20 GW/cm^2. The nonlinear surface susceptibility, which was defined earlier with respect to the laser fields external to the metal and the polarization sheet just inside the metal surface, was calculated using the model surface potential for gold described in Ref. 19, and was found to be $|\chi_s^{(2)}(\omega_3)| \simeq 4.6 \times 10^{-2}$ nm^2/V. It should be pointed out here that our calculated value is comparable to the experimental values in Refs. 15 and 16 for SHG. Under phase matching, the angular dependence of I_3 is given by the factor $|(1+\varrho_1)\sin\theta_1(1+\varrho_2^*)\sin\theta_2|^2$ that gives the shape of the main curve in the figure. The conversion efficiency $I_3/(I_1 I_2)^{1/2}$ at the peak of this curve is 3.5×10^{-8}. The inset shows the variation of I_3 with θ_2, while θ_1 is fixed to the optimal value

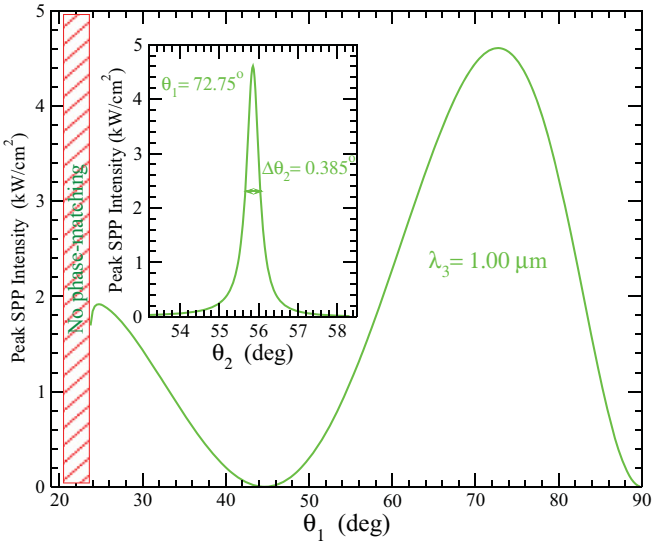

FIG. 4. (Color online) Plot of the peak SPP intensity vs the angle θ_1 along the corresponding phase-matching curve in Fig. 2, for $\lambda_3 = 1.00$ μm. The inset shows the peak SPP intensity vs the angle θ_2, with θ_1 fixed at the optimum value of 72.75 °.

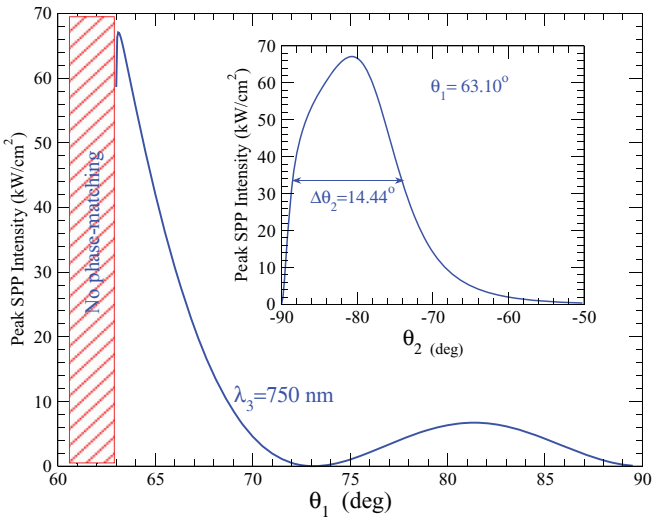

FIG. 5. (Color online) Plot of the peak SPP intensity vs the angle θ_1 along the corresponding phase-matching curve in Fig. 2 for $\lambda_3 = 750$ nm. The inset shows the peak SPP intensity vs the angle θ_2, with θ_1 fixed at the optimum value of 63.10 °.

of 71.50 °. In this case, the angular dependence is given by the factor $|(1+\varrho_2^*)\sin\theta_2|^2/[(\Delta k)^2+(k''_{spp})^2]$. The full width at half maximum (FWHM) of this angle tuning curve for phase matching is only $\Delta\theta_2 = 0.11$ °, and is determined essentially by the value of k''_{spp} ($L_{spp} = 294.3$ μm, $w = 1.3$ μm).

Similarly, Fig. 4 shows the dependence of the peak SPP intensity I_3 for $x \gg L_{spp}$ on the angle θ_1, for the points on the phase-matching curve in Fig. 2 corresponding to $\lambda_3 = 1.00$ μm. Our calculated value for the nonlinear surface susceptibility in this case is $|\chi_s^{(2)}(\omega_3)| \simeq 4.57\times10^{-2}$ nm^2/V, and the conversion efficiency at the peak of the curve is 2.3×10^{-7}. Note that there is also a second peak at (24.75 °, −69.17 °) with a peak plasmonic intensity of about 2 kW/cm^2. The inset shows the variation of I_3 with θ_2, while θ_1 is fixed to the optimal value of 72.75 °. At this shorter wavelength, the FWHM of the angle tuning curve for phase matching is $\Delta\theta_2 = 0.385$ °, which is broader than the previous case due to the larger value of k''_{spp} ($L_{spp} = 96.9$ μm, $w = 545$ nm).

Finally, Fig. 5 shows I_3 vs θ_1 for the points on the phase-matching curve in Fig. 2 corresponding to $\lambda_3 = 750$ nm ($L_{spp} = 31.7$ μm, $w = 267$ nm). For SPP excitation at this wavelength in the low-energy edge of the red region (620–750 nm) of the spectrum, the calculated value for the nonlinear surface susceptibility is $|\chi_s^{(2)}(\omega_3)| \simeq 6.7\times10^{-2}$ nm^2/V, and the conversion efficiency at the peak of the curve is 3.4×10^{-6}. This is two orders of magnitude greater than in the case of SPPs at the telecom wavelength. The inset shows I_3 vs θ_2, while θ_1 is held fixed to the optimal value of 63.10 °. In this case, the angle tuning curve is very broad, with a FWHM of $\Delta\theta_2 = 14.44$ °. This very large angular width is due mainly to the smallness of k_2 compared to k_1 ($k_2/k_1 \simeq 0.066$) and the very weak dependence of $k_{2x} = k_2\sin\theta_2$ on θ_2 in the range $-90° \leqslant \theta_2 \leqslant -70°$, making thus Δk rather insensitive to the variation of θ_2. As a consequence, the tuning curve is practically determined just by the factor $|(1+\varrho_2^*)\sin\theta_2|^2$, which gives this broad shape. Similar results have been obtained using $\lambda_1 = 620$ nm and $\lambda_2 = 5.0$ μm, generating SPPs at $\lambda_3 = 707.8$ nm. Neglecting bulk contributions, the calculated value for the surface nonlinear susceptibility is $|\chi_s^{(2)}(\omega_3)| \simeq 9\times10^{-2}$ nm^2/V, and the conversion efficiency reaches the value of 6×10^{-6}. We should mention here that the conversion efficiency for SPP excitation on a gold surface by DFG is two to three orders of magnitude larger than the efficiency for SHG in reflection from a gold surface.[19] This enhancement is not due to a significant difference in the $\chi_s^{(2)}$'s for the two processes, but just to the strong transverse confinement of the plasmonic field compared to the plane-wave front of the SHG field.

In conclusion, we have developed a theoretical description of the nonlinear optical excitation of SPPs by difference-frequency generation on a gold surface, and presented numerical calculations in the red and near-infrared region of the spectrum. The predicted conversion efficiency at 20 GW/cm^2 of laser pump intensities is four orders of magnitude larger than in recent experiments for SPP excitation at 633 nm by four-wave mixing. Higher conversion efficiency values are expected at shorter SPP wavelengths, before the efficiency will drop in the reflection edge of gold, in the yellow region of the spectrum.

*georges@danaos.physics.upatras.gr

[1] F. De Martini and Y. R. Shen, Phys. Rev. Lett. **36**, 216 (1976).
[2] J. Renger, R. Quidant, N. van Hulst, S. Palomba, and L. Novotny, Phys. Rev. Lett. **103**, 266802 (2009).
[3] N. Rotenberg, M. Betz, and H. M. van Driel, Phys. Rev. Lett. **105**, 017402 (2010).
[4] Chun-hua Xue, Hai-tao Jiang, and Hong Chen, Opt. Lett. **36**, 855 (2011).
[5] A. T. Georges, J. Opt. Soc. Am. B **28**, 1603 (2011).
[6] S. A. Maier, *Plasmonics: Fundamentals and Applications* (Springer, New York, 2007).
[7] K. F. MacDonald, Z. L. Samson, M. I. Stockman, and N. I. Zheludev, Nature Photon. **3**, 55 (2009).
[8] P. Vasa, C. Ropers, R. Pomraenke, and C. Lienau, Laser Photo. Rev. **3**, 483 (2009).
[9] Y. Wang, C.-Y. Lin, A. Nikolaenko, V. Raghunathan, and E. O. Potna, Adv. Opt. Photon. **3**, 1 (2011).
[10] P. Berini and I. De Leon, Nature Photon. **6**, 16 (2012).
[11] E. W. M. van der Ham *et al.*, J. Opt. Soc. Am. B **16**, 1146 (1999).
[12] Y. R. Shen, *The Principles of Nonlinear Optics* (Wiley, New York, 1984).
[13] J. A. Maytorena, W. L. Mochán, and B. S. Mendoza, Phys. Rev. B **57**, 2580 (1998).
[14] W. Hubner, K. H. Bennemann, and K. Bohmer, Phys. Rev. B **50**, 17597 (1994).
[15] D. Krause, C. W. Teplin, and C. T. Rogers, J. Appl. Phys. **96**, 3626 (2004).

[16]Fu Xiang Wang, F. J. Rodriguez, W. M. Albers, R. Ahorinta, J. E. Sipe, and M. Kauranen, Phys. Rev. B **80**, 233402 (2009).

[17]M. C. Gather, K. Meerholz, N. Danz, and K. Leosson, Nature Photon. **4**, 457 (2010).

[18]E. D. Palik, *Handbook of Optical Constants of Solids* (Academic, New York, 1985).

[19]N. E. Karatzas and A. T. Georges, J. Opt. Soc. Am. B **26**, 2218 (2009).